An application of profile fitting and CLAY++ for the quantitative representation (QR) of mixed-layer clay minerals

2 authors:

Patricia Aparicio
Universidad de Sevilla
87 PUBLICATIONS **727** CITATIONS

SEE PROFILE

Ray Ferrell
Louisiana State University
98 PUBLICATIONS **1,668** CITATIONS

SEE PROFILE

Some of the authors of this publication are also working on these related projects:

Project NASA EPSCoR View project

Project Mixed layer clay minerals View project

An application of profile fitting and CLAY++ for the quantitative representation (QR) of mixed-layer clay minerals

P. APARICIO[1],* AND R. E. FERRELL[2],†

[1] *Departamento de Cristalografía, Mineralogía y Q. Agrícola, Facultad de Química, Universidad de Sevilla, Apdo. 553, 41071 Seville, Spain, and* [2] *Department of Geology and Geophysics, Louisiana State University, E235 Howe Russell Geoscience Complex, Baton Rouge, LA 70803-4101, USA*

ABSTRACT: Clay mineral quantification by XRD is difficult when mixed-layer clay minerals and discrete clay types are both present. New procedures for peak decomposition and pattern simulation offer increased opportunities to obtain mineral abundance estimates. This proposed methodological sequence, for quantitative representation (QR) of complex clay samples, involves: (1) determination of layer type, mixed-layer proportion and order (R); (2) simulation of XRD patterns using MULCALC, an adaptation of NEWMOD; and (3) interpretation of the clay assemblage by fitting the whole pattern with CLAY++, a statistical program. The product is a QR of individual phases or a summation of layer types. The absence of quantitative reference standards means results cannot be checked for accuracy, but the statistical fit is highly reproducible and less prone to operator error. The QRs may be obtained with simulated or actual reference mineral patterns in the database. Results for freshwater marsh samples illustrate the approach.

One of the continuing challenges in the study of clay-rich materials is a quantitative analysis of the mineral assemblage by powder X-ray diffraction (XRD). The highly variable chemical and structural characteristics of clay minerals are major obstacles to their quantification. Other factors affect the XRD reflection intensities, such as the thickness of diffracting domains, particle thickness, particle-size distribution, and the sample weight or thickness in the holder. Sample preparation, the alignment of the X-ray instrument and data collection procedures may contribute significantly to the problem. These variables affect the reflection intensities of any component and make the selection of reference minerals very difficult (Brindley, 1980). The absence of certified standards and reference materials for the quantitative analysis of clay minerals is a critical issue. Accuracy is difficult to establish without them. A successful interpretation requires careful laboratory procedures with precise matching and standardization procedures. Even then, an accurate quantitative mineral analysis may be unattainable.

Moore & Reynolds (1997) raised the question "How good are quantitative analyses of clay minerals based on XRD?". If precision is the criterion, the answer is, "very good indeed". Thus, a set of replicate analyses may yield a relative standard deviation of perhaps $\pm 1.0\%$ (or less) of the amount present when the constituent minerals

are all present in reasonably large quantities, ~20 wt.% or more. But accuracy is another matter, because a carefully controlled quantitative analysis may still produce relative errors amounting to ±20% for minerals whose concentrations are near 20 wt.%. Thus, the numbers are only an approximation of the quantity present. Hughes *et al.* (1994) suggested the term "quantitative representation" (QR) to replace the traditional term, "quantitative phase analysis" (QPA); because QR represents the mineral content but does not imply an accurate measure of the absolute quantities present. With computerized methods for collection and manipulation of diffraction data, it may be possible to refine QR data to produce better QPA results (Hughes *et al.*, 1994). This paper describes a procedure to obtain a better QR.

In recent years, there have been improvements to facilitate quantification by XRD methods. Mudmaster (Eberl *et al.*, 1997), Decompxr (Lanson & Besson, 1992), Winfit (Krumm, 1996), MacXfit (Stanjek, 1995) and MacDiff 4.1.2 (Petschick, 2000) increase the ability to reduce overlapping peak interference and analyse peak shape to obtain more reliable intensity estimates. Details of the general decomposition approach were described by Lanson (1997). It can be applied to improve XRD results from a great variety of samples. Other computer programs such as NEWMOD (Reynolds, 1985), Interstrat (Garvie, 1994), MULCALC (Le & Ferrell, 1996), the Multispecimen method (Sakharov *et al.*, 1999), or Expert System (Plançon & Drits, 2000) have been developed to simulate XRD patterns or assist in the qualitative and quantitative analysis of clay mineral assemblages. Simulations reduce the need for actual standard minerals. Additional promising developments are computer programs to produce a statistical 'best-fit' of the entire XRD pattern instead of individual peaks (Ferrell *et al.*, 1992; Smith, 1992).

A recent example of the statistical 'best-fit' approach using the whole XRD pattern and a Rietveld procedure was provided by Jones *et al.* (2000). Basic structural and instrumental parameters were adjusted for crystalline components in several Hawaiian soils to calculate mass fractions. The preliminary results were then correlated with chemical analyses and additional XRD results following the addition of a corundum spike to obtain a QR of the minerals and amorphous materials present. This approach employs randomly oriented powders and does not account for mixed layering which may limit its application to more layer-silicate-rich clay materials.

Huang & Ferrell (1998) described a QR program, CLAY++, which uses simulated or pure mineral reference patterns for standardization and employs a statistical least-squares parameter to evaluate the fitting results. This program provides a better way to interpret clay mineral XRD patterns because it reduces operator-induced measurement and computation errors. Sample thicknesses obtained by applying >10 mg of clay/cm^2, highly oriented clay films, and standards most like the minerals present produce the best results. The most important benefits of this program are that it provides a quantitative representation (QR) of clay minerals present and an error estimator (R^2). R^2 is usually <0.01 when the computed and observed XRD patterns are almost identical. The use of the program is somewhat complicated because a large number of library patterns are frequently required to match the XRD pattern produced by a complex mineralogical sample, especially when several mixed-layer species are present in physical mixtures with the discrete clay types.

The aim of this work is to illustrate an improved methodological sequence for qualitative and quantitative representation of complex clay samples. It relies on the creation of an XRD library of representative pure clay and mixed-layer materials for use in the CLAY++ program. Profile-fitting procedures are employed routinely to reduce the number of reference profiles used in the quantitative procedure and to facilitate qualitative identification of phases present.

MATERIALS AND METHODS

Samples were collected from the freshwater marsh in the area of Lake Des Allemands near New Orleans (Louisiana, USA) from a depth of 200–206 cm (C1) and 290–300 cm (C9) respectively. The dark grey samples belong to the Kenner-Allemands soil association. They are typical of the moderately alkaline, fluid clays occurring beneath slightly acid mucks in freshwater marsh environments (McDaniel, 1987) of the Mississippi River Deltaic Plain.

Figure 1 shows the methodological sequence employed in the laboratory. The <2 μm and <0.2 μm fractions were extracted by normal settling and centrifugation techniques, respectively.
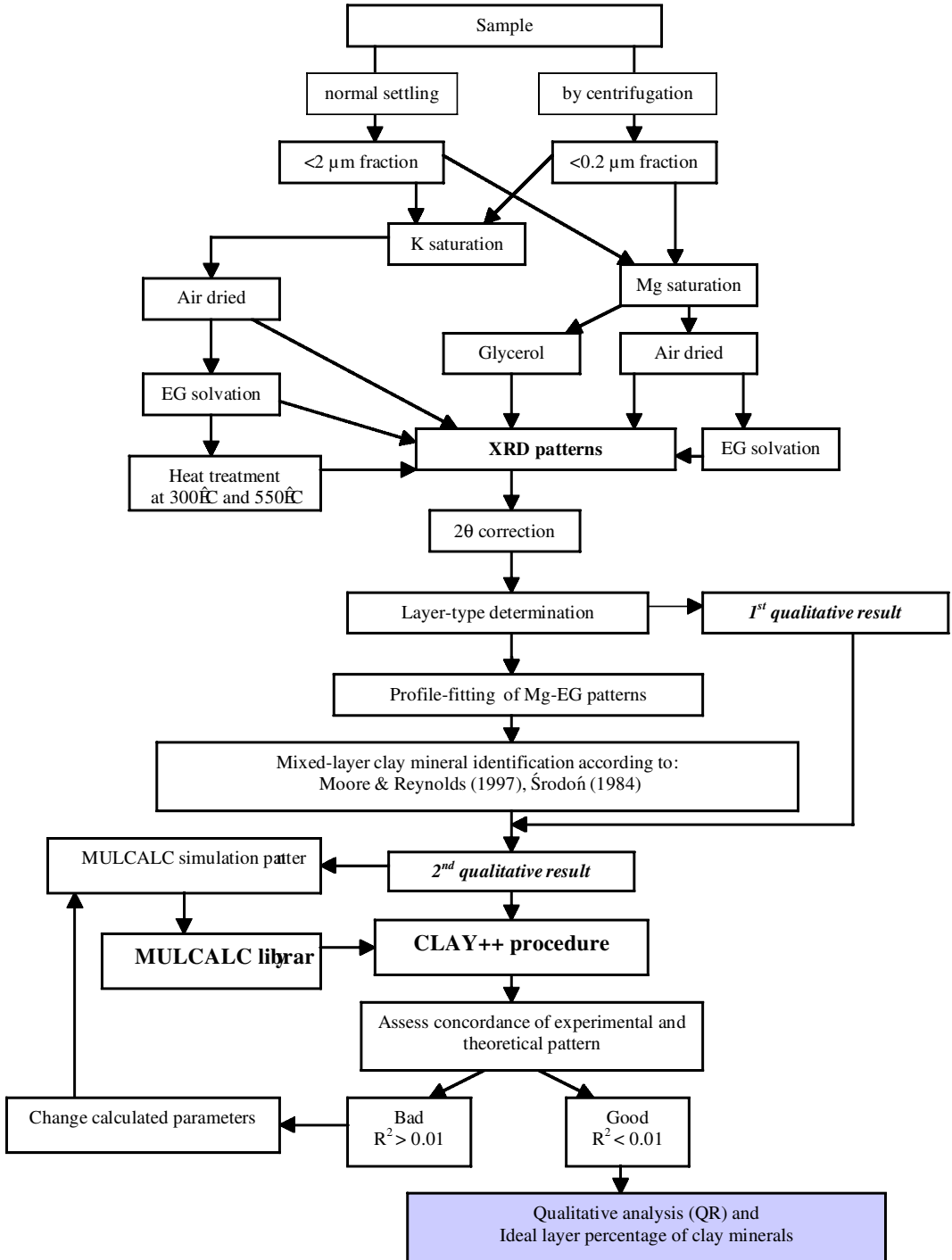
Fɪɢ. 1. Methodological sequence flow sheet.

Separate aliquots were saturated with Mg and K, and oriented films were produced by smearing a clay paste on glass slides to eliminate mineral segregation during slide preparation. Slides of Mg- and K-saturated samples were air dried and additional Mg-saturated samples were dried after saturating with glycerol (Dixon & White, 1995). X-ray diffraction traces of the air-dried slides were obtained after solvation with ethylene glycol (EG) and heat treatments (at 300°C and 550°C for 1 h) were performed on the K-saturated samples.

The XRD patterns were collected with Cu-$K\alpha$ radiation in a Siemens D5000 diffractometer at 40 kV, 30 mA, in the 2−36°2θ range. Counts were recorded at 0.02°2θ intervals for 1.0 s. A θ-compensating variable slit and sample spinning were used. The positions of reflections were corrected using the quartz (100) reflection as an internal standard. A profile-fitting peak decomposition program, part of MacDiff 4.1.2 by Petschick (2000), was used on the Mg-saturated and EG-treated sample patterns to determine the precise positions and intensities of the individual peaks within broad diffraction bands. A Pearson VII function was used, and the parameters obtained were: the peak position in °2θ, the height above the baseline, the full width at half height and the mixing parameter for the function. The initial fit results were iterated until the difference between the experimental and decomposed patterns was <5%.

Layer types in mixed-layer clay minerals were identified qualitatively with patterns obtained from Mg-saturated and glycerol-solvated samples, following the methods of Moore & Reynolds (1997) and Środoń (1984). Further identification was achieved by direct comparison with simulated diffraction profiles.

Simulation using MULCALC

MULCALC (Le & Ferrell, 1996) in C^{++} calculates the one-dimensional XRD patterns of mixed-layer clays using approaches adopted from NEWMOD (Reynolds, 1985). It was utilized to create patterns for pure clay minerals and two-component mixed-layer materials after changing the following variables: mixed-layer order (R), chemical composition of each layer, exchange cation, and other parameters related to crystallite-size distribution and the diffractometer. Simulations produced an XRD library of potential phases with peaks that matched the positions determined by peak decomposition.

Quantitative representation (QR) of the composition

CLAY++ (Huang *et al.*, 1993; Huang & Ferrell, 1998), a whole-pattern matching procedure, was used to calculate clay mineral percentages from XRD data. It determines the fractional contribution of patterns in the library database to the whole observed pattern by fitting with a least-squares minimization procedure. Mineral abundances are calculated by normalizing individual fractions to the sum of the fractional components and are expressed as weight percent of the crystalline fraction, thus ignoring contributions by amorphous organic and inorganic materials.

The 'goodness of fit' (R^2) is estimated in the matching procedure according to an intensity adjusted relationship (Howard & Preston, 1989), where:

$$R^2 = \{\Sigma(W_i(I_i^{obs} - I_i^{calc})^2)\}/\{\Sigma(W_i(I_i^{obs})^2)\}$$

$W_i = 1/I_i^{obs}$, for every °2θ data point. I^{obs} is the measured intensity of each XRD data point for the sample. I^{calc} is the sum of intensity contributions from each of the reference files. The formula for this calculation is:

$$I_i^{calc} = \sum_{h=0}^{n}(I_{ih} * MF_h)$$

Where I_{ih} is the intensity value (i) of reference file (h) in the library database, and MF_h is the weight contribution of the reference file (h). Iteration of MF_h by a trial-and error approach is performed for all library files until R^2 is at a minimum.

If the concordance between the observed and simulated pattern produces an unacceptable minimum, i.e. $R^2 > 0.01$, the reference database is changed. The most frequent changes are modifications to assumed chemical composition to match peak intensities or changes in crystallite size (coherent scattering domain) to match changes in peak width.

RESULTS

The mineral content of both samples is similar and the <0.2 μm fraction is simpler than the coarser fraction. The XRD patterns of sample C9 (290−300 cm) illustrate the changes produced by sample treatment procedures and provide the basis for the initial qualitative identification of the phases
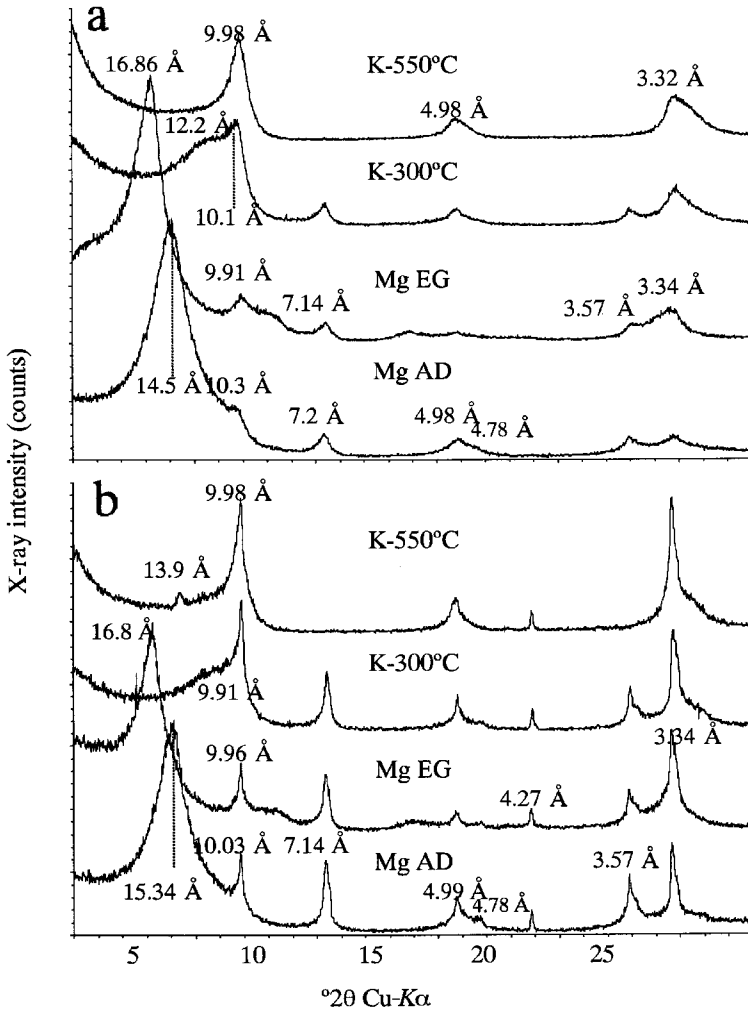
FIG. 2. Oriented aggregate pattern of sample C9 <0.2 μm fraction (a) and <2 μm fraction (b). Mg-saturated air-dried (Mg AD); Mg-saturated ethylene-glycol (Mg EG); K-saturated heat treatments at 300°C (K-300°C) and at 550°C (K-550°C).

present (Fig. 2). In the <0.2 μm fraction (Fig. 2a), a broad band at 14.5 Å in the Mg air-dried pattern expands to 16.9 Å with EG and several higher order reflections with *d* of 16.9 Å/*N* appear, indicating a high-swelling smectite. A 10.3 Å peak on the Mg air-dried pattern suggests the presence of an illite. A broad band at 7.2 Å, a 4.78 Å peak and the shoulder on the 3.57 Å peak indicate the presence of kaolinite and chlorite. K-saturation and heating to 300°C collapses some of the smectite layers to 10 Å and increases the 10.1 Å peak intensity. Some hydroxy-interlayers are indicated by the 12.2 Å

shoulder after 300°C treatment. All hydroxy-interlayers and kaolinite are destroyed by the 550°C treatment. The minerals present include illite, kaolinite, and a smectite with fully collapsed and partially collapsed interlayers, probably a high-charge and a low-charge smectite or a hydroxy-interlayered 2:1 clay mineral.

In the coarse clay fraction (<2 μm), the same minerals are present. Additional minerals include clay-sized quartz, chlorite and vermiculite. Chlorite is indicated by the more intense 4.78 Å and 3.53 Å peaks in the Mg air-dried pattern of Fig. 2b. The

distinct shoulder at 14.2 Å on the Mg-EG pattern and the 13.9 Å peak at the K-550°C pattern confirm the presence of chlorite. The presence of vermiculite is suggested by the refection at 14.12 Å on the Mg-glycerol pattern and at 11.54 Å on the heated K-glycerol pattern. Some potential for mixed-layering is indicated by the breadth of the peaks and the variation of the higher order peaks from a simple *d/N* sequence.

Peak decomposition (profile-fitting with MacDiff 4.1.2) reveals additional possibilities for qualitative consideration (Fig. 3). In the region from 24−28°2θ, the broad band with apparently 2 to 4 overlapping peaks may be simulated with six discrete peaks. The smoothed composite pattern produced by summing these simulated peaks produces a trace that closely approximates the average observed XRD intensity. The residual obtained by subtracting the measured from the calculated value exhibits about the same amount of variation due to noise and X-ray counting statistics as the original recording. A complete listing of the peaks derived by fitting the illustrated region and the entire background-subtracted pattern is compiled in Table 1 for the coarse and fine clay-fractions of sample C9. The values listed are possible positions that must be evaluated carefully to determine whether they represent rational or mixed-layer sequences produced by the minerals in the sample or are artifacts of the computation. The
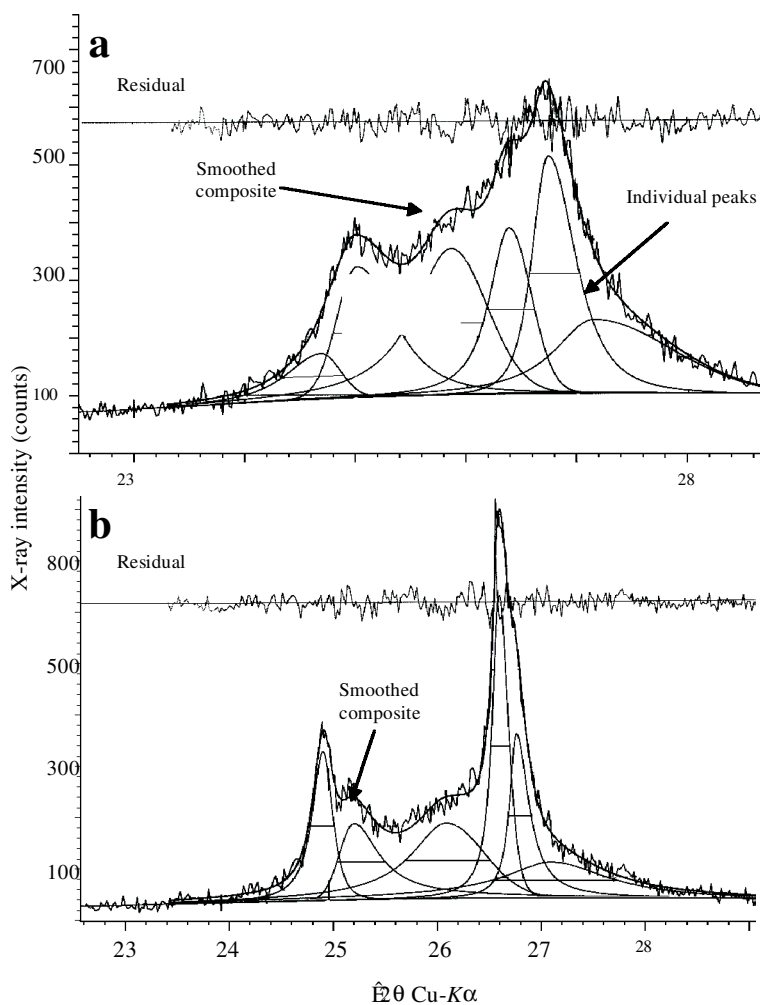

FIG. 3. Examples of peak decomposition results for C9 <0.2 μm fraction (a) and C9 <2 μm fraction (b).

TABLE 1. Decomposition results and peak identification possibilities for sample C9.

d_{hkl} (Å)	I (c)	H(Δ)	<2 μm Identification	I (c)	H(Δ)	<0.2 μm Identification
19.939	503	0.734				R0 illite (0.3)-smectite; R1 illite (0.1)-smectite
18.026	863	0.476				R1 illite (0.3)-smectite
16.749	959	0.50				R1 illite (0.5)-smectite
15.39	798	0.841				
13.612	343	1.202				R0 illite (0.2)-vermiculite; R0 illite (0.8)-vermiculite
10.721	192	0.941				
10.076	367	0.423	R0 illite (0.9)-smectite; R1 illite (0.9)-smectite	413	0.128	Illite
9.859	204	0.624				
7.3201	106	0.382				
7.1699	279	0.316	Kaolinite			Kaolinite
7.0391	52	0.319				
5.2184	63	0.898				
5.026	145	0.379		28	0.421	R1 illite (0.9)-smectite (?)
4.9358	168	0.438				Illite; R0 illite (0.2)-vermiculite
4.816	99	0.666				
4.6577	55	1.336				
3.6063	78	0.561				
3.5593	227	0.603	Vermiculite	44	0.228	Kaolinite
3.445	254	0.771		63	0.223	
3.3773	288	0.439	R1 illite (0.1)-smectite; R1 illite (0.3)-smectite			R1 illite (0.3)-smectite; R0 illite(0.3)-smectite; R1 illite (0.5)-smectite; R1 illite (0.1)-smectite; R0 illite (0.2)-vermiculite; R0 illite (0.8)-vermiculite
3.331	413	0.453	Illite			Illite; R1 illite (0.9)-smectite
3.2851	127	1.238				

peaks can be used to expand the qualitative possibilities described above.

Possible minerals associated with the *d*-values derived from profile-fitting are presented in Table 1. They were determined by comparison with published tables for discrete and mixed-layer clays (Moore & Reynolds, 1997; Środoń, 1984). The minerals detected in the initial qualitative analysis are still the most likely ones, but additional detail related to varieties of mixed-layer materials is provided. The 16.7−16.9 Å peak, for example, may now be attributed to an R = 0 smectite-illite with 0.6 to 0.7 smectite layers or an R = 1 smectite-illite with 0.9 smectite layers. Additional peaks at smaller *d* values agree in part with this interpretation. Unidentified peaks probably represent artifacts of the decomposition procedure. Identifications in Table 1 provide the basis for the selection of patterns to include in the library database used in CLAY++. Present limitations restrict the analysis to 15.

CLAY++ results for samples C1 and C9 are presented in Table 2. The best fit of the fine clay-

TABLE 2. Mixed-layered proportion, ordering and QR (wt.%) results obtained with CLAY++.

Sample	R^2	Phases presented (low N, high N)	Dimica Fe	Dimica K	Dismectite Fe	Divermiculite Fe	wt.%
					Clay composition		
		Illite (3, 14)	1	0			6.5
		Illite (10, 20)	1	1			1.2
C1		Kaolinite (20, 30)					4.6
200−206	0.017	Smectite (3, 14)			1.5		8.7
<0.2 µm		R0 illite (0.5)-smectite (2, 3)	0.5	1	0.5		49.1
		R0 smectite (0.7)-illite (2, 3)	0.5	1	0.5		14.9
		R0 illite (0.9)-smectite (2, 3)	0.5	1	0.5		15.0
		Chlorite * (3, 14)					7.2
		Illite (3, 14)	1	0			0.5
		Illite (10, 20)	1	1			13.1
C1		Kaolinite (20, 30)					8.0
200−206	0.009	Smectite (3, 14)			1.5		3.6
<0.2 µm		Vermiculite (3, 14)				1.5	1.6
		R1 smectite (0.7)-illite (2, 3)	0.2	1	0.2		32.8
		R1 illite (0.9)-smectite (3, 14)	1	1	1		14.8
		R1 smectite (0.9)-illite (3, 14)	1	1	1		12.3
		R1 illite (0.6)-vermiculite (3 ,14)	1	1		1	4.1
		Quartz					2.0
C9		Illite (3, 14)	1.5	1.0			13
290−300	0.010	Kaolinite (10, 20)					3.7
<0.2 µm		Smectite (3, 14)			1.5		7.3
		R1 smectite (0.7)-illite (2, 3)	0.2	1	0.2		53
		R0 illite (0.9)-smectite (2, 3)	0.5	1	0.5		23
		Chlorite* (3, 14)					5.2
		Illite (3, 14)	0	0.5			6.3
		Illite (15, 32)	1	0			8.1
C9		Kaolinite (20, 30)					10.4
290−300	0.012	Smectite (3, 14)			1.5		8.6
<0.2 µm		Vermiculite (3, 14)				1.5	1.8
		R1 smectite (0.7)-illite (2, 3)	0.2	1	0.2		20.1
		R0 illite (0.9)-smectite (2,3)	0.5	1	0.5		26.4
		R0 vermiculite (0.8)-illite (3, 14)	1	1		1	9.7
		Quartz					3.4

* The chlorite used was trichlorite-trichlorite with Fe(1) = 2, Fe(2) = 0 and OH = 1

fraction of sample C1 employed a tri-tri chlorite, kaolinite, smectite, two varieties of illite, two randomly mixed-layer smectite-illites, and a randomly mixed-layer illite-smectite. Only five clay minerals were obtained from the analysis of the fine clay fraction of sample C9. The composition of the chlorite and other minerals plus *N* values (crystallite thickness) used to produce the patterns used in the match are also listed. All analyses incorporated the XRD scan of a blank glass plate as a way to account for scattering from amorphous material. Weight percent values were obtained by normalizing the mineral multiplication factors to 100.

The most abundant mineral in the fine clay fraction of samples C1 and C9 is a smectite-illite (Table 2). In C1, it is a randomly interstrafied mineral with equal proportions of smectite and illite layers representing ~46 wt.% of the <0.2 μm fraction. In C9, the smectite-illite is ordered with 0.7 smectite layers and represents 53 wt.% of the sample. Both have a moderate Fe content and one K atom in the interlayer of the illite packets. The next most abundant minerals are other varieties of smectite-illite and illite-smectite. Total smectite layers represent 57 and 65 wt.% of samples C1 and C9, respectively (Table 3).

The mineral composition of the coarse clay fraction is different from the fine clay. New minerals detected included quartz, chlorite, vermiculite and ordered illite-vermiculite. Ordered smectite-illite and illite-smectite with slightly different fractions of illite layers provided a better match with the coarse clay patterns. The sum of ideal layer percentages (Table 3) indicates more total smectite in the fine clay and more kaolinite, chlorite and vermiculite layers in the coarse clay. Illite layer totals are approximately the same.

In the coarse clay-fraction of C1, the most abundant mineral (32.8 wt.%) is the same as in the coarse clay fraction of C9, an ordered smectite-illite with 0.7 smectite layers. In the coarse clay of C9, a randomly interstratified illite-smectite with 0.9 illite layers is the second most abundant mineral (26 wt.%). The illite and smectite layers in the coarse clays also have higher Fe contents than in the finer clays (Table 2). Many of the other simulated clay minerals had relatively high Fe contents. The best match for chlorite diffraction peaks was obtained when the interlayer hydroxide sheet was complete and when both trioctahedral hydroxide sheets contained 2.0 Fe atoms. For illite, several variations with different K and Fe contents were utilized. When vermiculite was required in the matching process it was dioctahedral in character and contained the equivalent of 1.0−1.5 Fe atoms.

DISCUSSION

A general appraisal of the QR produced by whole-pattern fitting can be obtained by comparison of the experimental XRD pattern with the composite one generated by CLAY++ (Fig. 4). For the fine clay there is a general agreement throughout the interval from 4−30°2θ. For the coarse clay-fraction, the calculated and experimental pattern intensities are also very similar except for the area near the 5 Å peak and the region near 3.34 Å. The R^2 values for these patterns are 0.012 and 0.010, respectively. The matches based on the presence of 6 to 11 clay minerals appears to duplicate reasonably the XRD pattern produced by these mineralogically complex samples from the Mississippi River Drainage Basin. The fine clay fractions should also be simpler than the coarse fraction as indicated. The results are very reproducible because multiple runs yield identical results as long as the reference library does not change. The sensitivity is limited to 1.0 wt.% by the step restrictions in the CLAY++ iteration procedure.

There are several opportunities in the interpretation procedure to improve the results. The two stages of

TABLE 3. Quantitative representation (%) of ideal layer types.

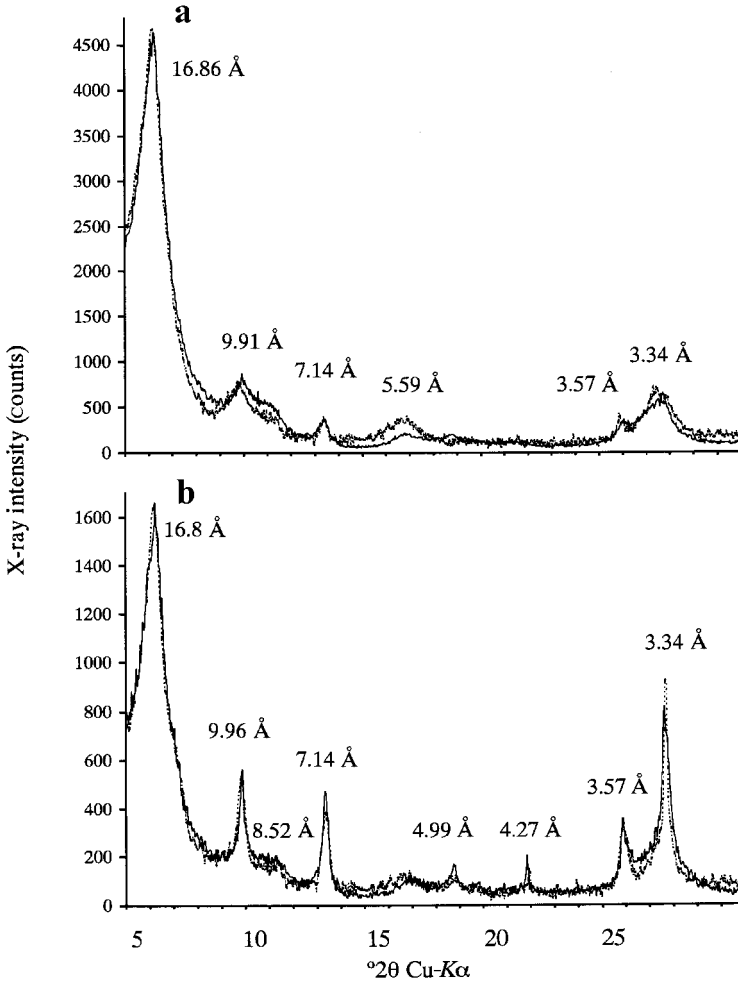| Sample		Quartz	Kaolinite	Illite	Smectite	Chlorite	Vermiculite
C200−206 cm	<2 μm	2.0	8.0	40.4	39.2	7.2	3.2
	<0.2 μm	−	4.6	38.7	56.7	−	−
C290−300 cm	<2 μm	3.4	10.3	25.0	46.5	5.2	9.5
	<0.2 μm	−	3.7	31.2	65.1	−	−

FIG. 4. Experimental (solid) and simulated (dashed) X-ray pattern for sample C9. (a) <0.2 μm fraction and (b) <2 μm fraction.

qualitative interpretation, one with peak decomposition, follow standard procedures for visual inspection and identification of clay mineral assemblage in soils and sediments. The recognition of individual peaks in broad diffraction bands increases the ability to identify more mineral varieties in a complex mixture. Interpreting the fine clay before the coarse clay makes common components easier to recognize because the former size fraction is usually less complex. The detailed results for the two samples described above illustrate how much more information can be obtained. A broader indication of the applicability is available in Dypvik & Ferrell (1998) where different varieties of smectites were recog-

nized in normal marine sediments and ejecta from the Mjolnir crater.

Whole-pattern fitting has recognizable advantages because the QR is not based on single-peak intensity values. This approach also makes it possible to produce information about the composition of clay layers. As illustrated in Fig. 5, the initial match based on peak position yields limited concordance of peak intensities and peak widths. The minimal R^2 produced by this analysis is moderately good, but visual inspection (Fig. 5a) shows that the interpretation is open to question. There are many areas where the profiles are noticeably different. The agreement can be
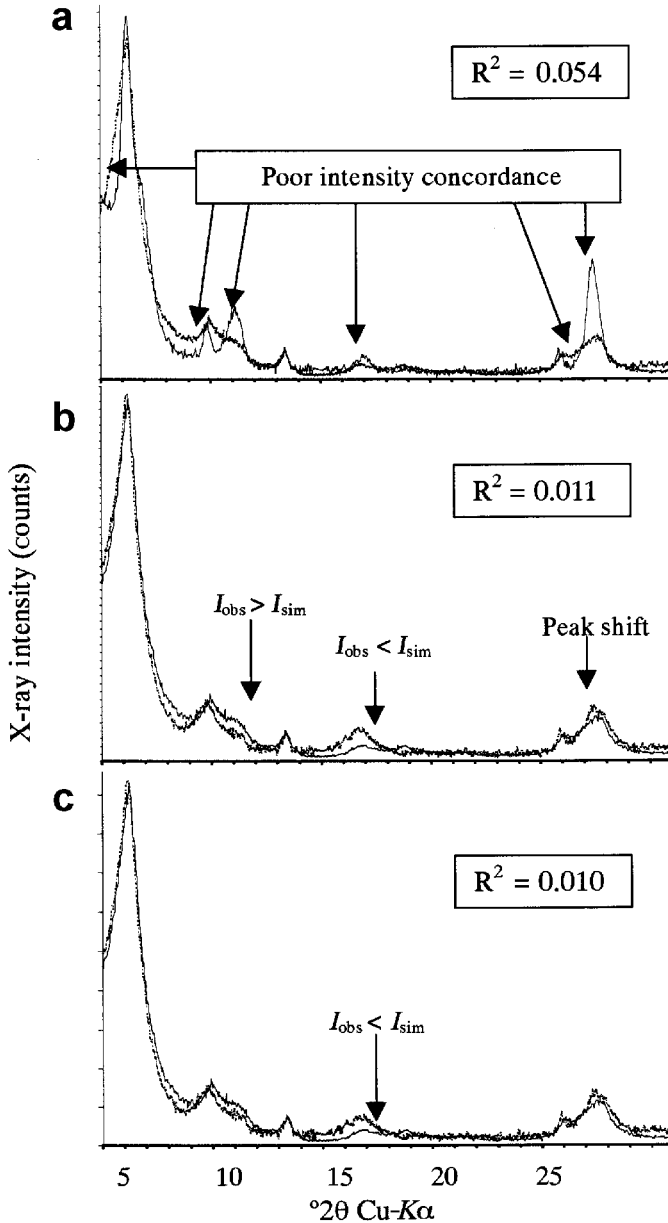
FIG. 5. Improvement in concordance of simulated and experimental XRD patterns of the <0.2 μm fraction of C9 achieved by varying the layer composition of illite and smectite. (a) Fe content of 1.0 in illite and smectite layers; (b) after increasing Fe to 1.5 in illite and decreasing Fe in R1 smectite (0.7, 0.9)-illite to 0.2; (c) best agreement obtained for further reducing Fe in R1 illite (0.1)-smectite to 0.5.

improved (Fig. 5b) by increasing the Fe content of illite to 1.5 and decreasing the Fe content of illite and smectite in R1 smectite-illite with 70% and 90% smectite layers, but there are at least three

areas where the intensities are still noticeably different. A further reduction in the Fe content of smectite and illite to 0.5 atoms per half unit cell reduces R^2 to 0.010 and produces the patterns

illustrated in Fig. 5c. There are still small discrepancies in the observed and simulated intensities that are virtually impossible to eliminate. They are attributed to differences in the crystallite orientation and other parameters related to specimen preparation and data collection that cannot be evaluated directly.

The question "How good is the procedure for quantitative analysis of clay-rich samples?" remains unanswered. It may never be answered because quantitative analysis standards for clay minerals are not available and probably never will be. The utility of this procedure is best demonstrated when discussed in terms of a QR. The goal of a QR analysis to generate a reproducible numerical representation of the clay assemblages is clearly demonstrated by this approach. The use of simulated patterns, peak decomposition procedures to assist with qualitative identification, and a mathematical fitting procedure produce a numerical estimate of the components in the clay assemblages that is very reproducible and provides more detail on the types of mixed-layer minerals present than conventional methods.

The success of this approach relies on good laboratory procedures. Reproducibility is very dependent on producing uniformly thick samples with a high degree of preferred orientation, because the simulations incorporate peak width factors. If good orientation is not achieved, the decomposition and crystallite thickness aspects of the analysis may become meaningless. A variably thick sample prohibits the matching of whole-pattern peak intensities. The small areas, where simulated and experimental patterns fail to agree (Fig. 5c), may be the results of orientation effects.

Common sense is an important ingredient of any interpretation and one must always assess results to determine if they are reasonable with respect to the origin and properties of the materials being analysed. Including a large number of variables (phases) may produce an exaggerated 'goodness of fit'. In this procedure, visual appraisal of the match results and the fact that CLAY++ often returns a fit that does not employ all reference files in the database are positive indications of a common-sense fit.

However, there are some characteristics of the simulated profiles that raise concern. The suggested presence of R = 1 smectite-illite with 0.7–0.9 smectite layers in the assemblage is one of these. Ordering is not usually reported in a mixed-layer

illite and smectite until the fraction of illite layers exceeds 0.5. The observed diffraction effects may be the results of three-component mixed layering or the production of hydroxy interlayers with EG-saturated spacing >17 Å.

The reported clay mineral assemblages call attention to the complex mineralogy of sediments and soils. The various minerals are all potentially present considering the alteration that may be occurring in the present-day environment and the variability of source materials contributed by the Mississippi River and its tributaries. Differences in the quantities of vermiculite-like materials in the coarse and fine fractions of both materials might be attributable to hydroxy-interlayer formation and crystallite growth. Additional work is in progress to relate these mineralogical results to the chemical composition of individual particles determined by electron microprobe analysis and ion exchange properties of the samples.

CONCLUSIONS

The methodological sequence proposed above is an improvement over others because it combines traditional procedures with the use of simulated XRD patterns, decomposition procedures for qualitative identification, and a mathematical fitting procedure to obtain a QR of complex clay assemblages.

The QR results based on the presence of 6–11 clay minerals are reasonable with respect to the origin and properties of the materials.

The proposed method yields a reproducible numerical estimate of the components in clay mineral assemblages but is not a truly quantitative analysis. Accuracy cannot be evaluated due to the absence of reference standards.

The results provide more details than conventional methods on the types of mixed-layer minerals present.

The success of this approach relies on good laboratory procedures and common sense in the selection of minerals to include in the reference database.

DISTRIBUTION OF CLAY++ AND XRD PATTERNS LIBRARY

CLAY++ and the XRD library patterns are available from the authors. CLAY++ requires a PC with Windows 95, or higher.

REFERENCES

Brindley G.W. (1980) Quantitative X-ray mineral analysis of clays. Pp. 411−438 in: *Crystal Structures of Clay Minerals and Their X-ray Identification* (G.W. Brindley & G. Brown, editors). Monograph, **5**. Mineralogical Society, London.

Dixon J.B. & White G.N. (1995) *Soils Mineralogy Laboratory Manual*. Agronomy, **626**. Available from J.B. Dixon, Department of Soil Crop Sciences, Texas A&M University, College Station, TX, 77843-2474, USA.

Dypvik H. & Ferrell R.E. (1998) Clay mineral alteration associated with a meteorite impact in the marine environment (Barents Sea). *Clay Miner.* **31**, 51−64.

Eberl D.D., Drits V., Środoń J. & Nüesch R. (1997) *MudMaster, a program for crystallite size distribution and strain from the shape of XRD diffraction pattern*. Available from the US Geological Survey at ftp://brrcrftp.cnr.ugs.gov/ pub/ddeberl

Ferrell R.E., LaMotte L.R., LeBlanc W.S., Wilensky D.E. & Mao L. (1992). "Whole pattern" XRD interpretation of mineralogical variation. Pp. 673−679 in: *Advances in X-ray Analysis* (C.S. Barrett, J.V. Gilfrich, T.H. Huang, R. Jenkins, G.J. McCarthy, P.K. Predecki, R. Ryon & D.K. Smith, editors). Plenum Press, New York.

Garvie L.A.J. (1994) Interstrat – an expert system to help identify interstratified clay minerals from powder XRD data: II. Testing the program. *Clay Miner.* **29**, 21−32.

Howard S.A. & Preston K.D. (1989) Profile fitting of powder diffraction patterns. Pp. xxx−xxx in: *Modern Powder Diffraction* (D.L. Bish & J.E. Post, editors). Reviews in Mineralogy, **20**. Mineralogical Society of America, Washington, D.C.

Huang K. & Ferrell R. (1998) ***Clay***++*: A computer program for quantitative clay mineral analysis*. Department of Geology and Geophysics E235 Howe/Russell Geoscience Complex, Baton Rouge, LA 70803, USA.

Huang K., Ferrell R.E. & LeBlanc W.S. (1993) Computer assisted interpretation of clay mineral diffraction patterns. *30th Annual Meeting of the Clay Minerals Society*, San Diego, p. 51.

Hughes R.E., Moore D.M. & Glass H.D. (1994) Qualitative and quantitative analysis in soils. Pp. 330−359 in: *Quantitative Methods in Soil Mineralogy* (J.E. Ammonette & L.W. Zelazny, editors). SSSA Miscellaneous publication. Soil Science Society of America, Inc. Madison, Wisconsin, USA.

Jones R.C., Babcock C.J. & Knowlton W.B. (2000) Estimation of the total amorphous content of Hawai'I soils by the Rietveld method. *Soil Sci. Soc. Am. J.* **64**, 1100−1108.

Krumm K. (1996) *Winfit. A Windows program providing an interface for single or multiple curve fitting*. Available from the author at ftp://xray.geol.uni-erlangen.de/ software.

Lanson B. (1997) Decomposition of experimental X-ray diffraction patterns (profile fitting): A convenient way to study clay minerals. *Clays Clay Miner.* **42**, 132−146.

Lanson B. & Besson G. (1992) Characterization of the end of smectite-to illite transformation: Decomposition of the X-ray patterns. *Clays Clay Miner.* **40**, 40−52.

Le T.H. & Ferrell R. (1996) *MULCALC*. Department of Geology and Geophysics E235 Howe/Russell Geoscience Complex, Baton Rouge, LA 70803, USA.

Mc Daniel D. (1987) *Soil Survey of St. Charles Parish, Louisiana*. United States Department of Agricultural, Soil Conservation Service, 115 pp.

Moore D.M. & Reynolds R.C. (1997) Quantitative analysis. Pp. 298−329 in: *X-ray Diffraction and the Identification and Analysis of Clay Minerals*, (second edition). Oxford University Press, Oxford and New York.

Petschick R. (2000) MacDiff 4.1.2. Powder diffraction software. Available from the author at http://www.geol.uni-erlangen.de/html/software/Macdiff.html.

Plançon A. & Drits V. (2000) Phase analysis of clays using a expert system and calculation programs for X-ray diffraction by two and three component mixed-layered minerals. *Clays Clay Miner.* **48**, 57−62.

Reynolds R.C. (1985) *NEWMOD, a computer program for the calculation of one-dimensional diffraction patterns of mixed layered clays*. R.C. Reynolds, 8 Brook Drive, Hanover, New Hampshire 03755, USA.

Sakharov B.A., Lindgreen H., Salyn A. & Drits V. (1999) Determination of illite-smectite structures using multispecimen X-ray diffraction profile fitting. *Clays Clay Miner.* **47**, 555−566.

Smith D.K. (1992) Particle statistics and whole-pattern methods in quantitative X-ray powder diffraction analysis. Pp. 1−15 in: *Advances in X-ray Analysis* (vol. **35**) (C.S. Barrett, J.V. Gilfrich, T.H. Huang, R. Jenkins, G.J. McCarthy, P.K. Predecki, R. Ryon & D.K. Smith, editors). Plenum Press, New York.

Środoń J. (1984) X-ray powder diffraction identification of illitic materials. *Clays Clay Miner.* **32**, 337−349.

Stanjek H. (1995) *MacXfit. X-ray diffraction profile fitting program for Macintosh v.1.1.5a.* Developed by Helge Stanjek, TU Munich, Germany. Available from the author at e-mail: stanjek@weihenstephan.de .